ON THE OPTICAL SPECTRUM OF MU CEPHEI

Tõnu Kipper

Tartu Observatory, Tõravere, 61602, Estonia; tk@aai.ee

Received: 2010 September 16; accepted 2010 October 4

Abstract. High resolution spectra of M-type supergiant μ Cep are analyzed. The movements in the atmosphere of this star are highly supersonic and variable with depth. The lines forming in deeper layers show the widths corresponding to $30~{\rm km\,s^{-1}}$. The lines forming in outer layers are much wider, $50~{\rm km\,s^{-1}}$. At the same time, the microturbulent velocity ($\xi_{\rm t}$) is low, from 4.0 to 4.5 km s⁻¹. The atmosphere of μ Cep is slightly metal deficient with [Fe/H] \approx -0.4.

Key words: stars: atmospheres – stars: individual: μ Cep

1. INTRODUCTION

Herschel's Garnet Star, μ Cephei is one of the largest and most luminous stars in the Milky Way (Humphreys 2007). It belongs to red supergiants (RSG) which are evolved massive ($M_{\rm init}=10$ to $25\,M_{\odot}$) stars burning helium in their cores (Massey et al. 2008). Their spectra show strong line broadening which seems to be different for different lines. The atmospheric dynamics of μ Cep and other red supergiants was studied recently by Josselin & Plez (2007) using the tomography technique. In this note we analyze the same observational data by more traditional approach. We use the concept of the line formation depth instead of mere line center optical depth for characterizing the atmospheric dynamics. We will also try to determine the still poorly known chemical composition of μ Cep.

The spectra of μ Cep were taken from the ELODIE archive (Moultaka et al. 2004). Overall 20 spectra, observed by Eric Josselin from 1999 to 2004, were used. The spectra cover the wavelength region 400–680 nm with S/N=100 to 350 at 550 nm and a wavelength resolution of 0.0132 nm.

For the present analysis all the spectra were preliminary coadded. Before that they were shifted in the wavelength using as a zero-point the spectrum obtained on JD 2453211.5. The shifts were found by cross-correlating the spectra.

2. ANALYSIS

2.1. Atmospheric parameters and model atmospheres

The known atmospheric parameters of μ Cep are listed in Table 1. The effective temperature is known rather well. The older temperature scale for RSGs indicated too low temperatures, and their location in the HR diagram was in disagreement with the evolutionary tracks (Massey et al. 2007). Using the new generation MARCS atmospheric models (Gustafsson et al. 2003) for fitting the TiO bands

allowed to Levesque et al. (2005) to solve this problem and to establish a new temperature scale for RSGs. For μ Cep Levesque et al. (2005) have found $T_{\rm eff}=3700~{\rm K}$. Josselin & Plez (2007) used the V-K color and $T_{\rm eff}$ calibration by Bessell et al. (1998) to find $T_{\rm eff}=3750~{\rm K}$.

Table 1. Basic parameters of μ Cep (HD 206936).

Sp.	Var.	V	B– V	V– K	E_{B-V}	A_V	$T_{ m eff}$	$\log g$	$M_{ m bol}$
M2 Iab	SRc	4.08 4.02	2.35	5.96 5.90	0.66 ± 0.19	2.01	0.00	-0.5 -0.36	-9.08 -8.88

In the first line the data from Levesque et al. (2005) and in the second line the data from Josselin & Plez (2007) are given.

When fitting the spectra, the surface gravity for RSGs was chosen by Levesque et al. (2005) iteratively starting with $\log g = -0.5$ which corresponds to $M_{\rm bol}$ and the old temperature scale. With the new scale they found that $\log g = 0$ was more consistent with the RSGs locations in the HR diagram. Levesque et al. (2005) also found that the choice of $\log g$ has affected the derived values of E_{B-V} by < 0.1 mag and had no effect on the derived effective temperatures. Josselin & Plez (2007) for μ Cep found $\log g = -0.36$ on the basis of adopted $M_{\rm bol} = -8.88$ and the $25 M_{\odot}$ mass. According to these data, I started the analysis with $T_{\rm eff} = 3700$ K. The constant surface gravity $\log g = 0.0$ was chosen.

The models were taken from the Plez (1992) grid. These are the same models which were used by Levesque et al. (2005). There is no model with $T_{\rm eff}=3700~{\rm K}$ in the grid. Therefore I interpolated the temperature at a given gas pressure in the models (3600/0.0) and (3800/0.0) corresponding to 5 M_{\odot} . This mass is lower than is expected for μ Cep but the $T(p_g)$ distribution of plane-parallel atmospheric models depends on the stellar mass through $\log g$, which was fixed as described earlier. Later (see section 2.3), when deriving the Ti abundance, we found that $T_{\rm eff}$ should be lowered by 100 K and therefore we used the model (3600/0.0) afterwards.

2.2. Measurement of the spectra

The coadded spectrum was normalized to a continuum using the IRAF task 'continuum', and the wavelengths, equivalent widths and half-widths (FWHW) of lines were measured with the task 'splot', which was also used to decompose the blends. This was reasonably possible down to the wavelength of ~ 480 nm. However, most of the measured lines were severely blended and during the subsequent analysis were rejected. The element abundances and the line formation depths were calculated with the code WIDTH5 (Kurucz 1979). The solar oscillator strengths by Thevenin (1989, 1990) were used.

The FWHW of lines were found to be dependent on line strength. In Figure 1 the dependence of line widths on the formation depth is shown. In the code WIDTH5 the line formation depth is calculated as weighted over the line profile mass depth $\rho_{\rm x}$ corresponding to the monochromatic optical depth 1 ($\rho_{\rm x} = P_{\rm tot}(\tau_{\lambda}=1)/g$).

Figure 1 shows that the lines forming in the highest layers are widened by the motions with 50 km s^{-1} velocities while in the deepest layers the observed velocities are 30 km s^{-1} .

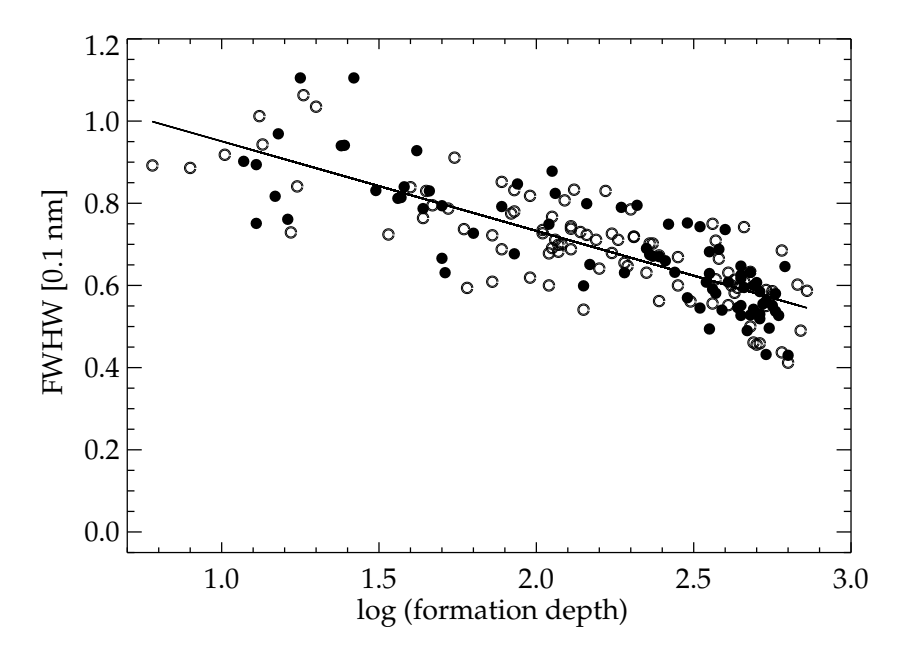


Fig. 1. The dependence of line widths (FWHW) on the formation depth. The Fe I lines are plotted as filled dots, the lines of other elements (Ti I, Cr I, Mn I, V I, Ni I,Ca I and Ba II) as open circles. The line is drawn by the least-square fit for all lines.

2.3. Chemical composition

Abundance analyses for M supergiants are rare. The first attempt to find the chemical composition of μ Cep was by Yamashita (1956, 1965) using the curve-of-growth method for the S-S atmospheric model. He was able to found the abundances of some elements relative to neutral iron. He obtained the excitation temperature 2800 K and the microturbulent velocity 9.3 km s⁻¹. A few years later Orlov (1967) did the same with the M-E type curve-of-growth. He found the abundances of several elements relative to iron which are, however, quite different from the solar values. He also adopted $T_{\rm exc}=2800$ K and get the microturbulent velocity $\xi_{\rm t}=15~{\rm km\,s^{-1}}$.

When deriving the new temperature scale for red supergiants by TiO band strengths, Levesque et al. (2005) used the solar metallicity and presumably the solar oxygen abundance. The abundances of Ti, O and C have strong effect on the TiO band strength. We assumed $\log\varepsilon({\rm O/H})=8.80$ according to findings by Lambert et al. (1984) for another M-type supergiant, Betelgeuse. With this oxygen abundance and $\log\varepsilon({\rm C/H})=8.52$ and $\log\varepsilon({\rm Ti/H})=4.90$, the TiO bandheads at 516, 545, 585, 616, 658–680 nm are well reproduced in the synthetic spectra (visual inspection). In the spectrum synthesis, the lists of Bell (1976) for metallic lines and of Plez (1998) for TiO lines were used. A good fit was obtained when differences in abundances do not exceed $\pm\,0.1$ dex in both O and Ti and $\pm\,0.05$ dec in C. However, the Ti abundance derived from the equivalent widths was found to be lower by about 0.4 dex (see below). This means, that in order to preserve the same TiO band strengths with the same oxygen and carbon abundances, the temperature should be lowered to $T_{\rm eff}=3600$ K. This temperature was used in

the subsequent abundance analysis. The choice of O and C abundances affects only the strength of TiO bands, with no effect on the derived abundances of other elements.

Table 2. Chemical composition of μ Cep. The number of used lines is indicated in remarks. The microturbulent velocity $\xi_{\rm t} = 4.0~{\rm km\,s}^{-1}$ was used in all cases.

	Sun^1	μ Pe		
El.	$\log \varepsilon$	$\log \varepsilon$	[El/Fe]	Remarks
H	12.00			
$^{\rm C}$	8.55	8.52	0.38	Input abund.
O	8.87	8.80	0.34	Input abund.
Na	6.33	6.76 ± 0.24	0.84	2 Na I
Mg	7.58	6.39 ± 0.66	-0.78	3 Mg I
Si	7.55	7.63 ± 0.00	0.49	5 Si I
Ca	6.36	5.99 ± 0.29	0.43	12 Ca I
Sc	3.17	2.17 ± 0.33	-0.59	5 Sc I, 1 Sc II
Ti	5.02	4.40 ± 0.27	-0.21	19 Ti I
V	4.00	3.41 ± 0.29	-0.18	14 V I
Cr	5.67	4.92 ± 0.34	-0.34	21 Cr I
Mn	5.39	4.84 ± 0.30	-0.14	7 Mn I
Fe	7.50	7.09 ± 0.20		57 Fe I
Со	4.92	4.53 ± 0.24	0.02	4 Co I
Ni	6.25	6.10 ± 0.39	0.18	14 Ni I
Cu	4.21	4.74 ± 0.19	0.94	3 Cu I
Y	2.24	2.10 ± 0.15	0.27	2 Y II
Zr	2.60	1.21 ± 0.36	-0.98	5 Zr I
$_{\mathrm{Ba}}$	2.15	2.59 ± 0.12	0.27	3 Ba II
Sm	1.01	1.09 ± 0.54	0.49	2 Sm II

¹ Grevesse et al. (1996), relative to $\log \varepsilon(H)$.

We started the analysis with Fe I for which the largest number of comparatively unblended lines was found. In Figure 2 the derived iron abundances are plotted versus $\log(EW/\lambda)$ for 80 Fe I lines. The needed microturbulent velocity is $4.5~{\rm km\,s^{-1}}$ and the iron abundance is $\log \varepsilon(\text{Fe}) =$ 6.99 ± 0.24 . The scatter is large and there is some irregularity in the distribution of points at $\log(EW/\lambda) = -1.2$. In Figure 3 the line formation depths are plotted against $\log(EW/\lambda)$. Here one could notice that at this value of the reduced equivalent width the dependence starts to diverge and for stronger lines it splits into two branches. This behavior is related to the way how the formation depth is calculated. For broader lines the difference in the formation depths of the line core and wings starts to show up and for

very broad lines the contribution of wings takes over. Therefore we have set a limit $\log(EW/\lambda) \le -1.2$ for the abundance analysis.

The results are shown in Figure 4. We get the microturbulent velocity $\xi_{\rm t}=4.0~{\rm km\,s^{-1}}$ and the iron abundance $\log \varepsilon({\rm Fe})=7.09\pm0.20$ from 57 Fe I lines. When treated separately, the stronger lines give very close abundance, $\log \varepsilon({\rm Fe})=7.14\pm0.23$, with a slightly higher $\xi_{\rm t}=4.3~{\rm km\,s^{-1}}$.

For Ti I only 19 lines were found and with $\xi_t = 4.0 \text{ km s}^{-1}$ the titanium abundance is $\log \varepsilon(\text{Ti}) = 4.40 \pm 0.27$.

No Li I line at 670.8 nm was found.

The summary of abundances is presented in Table 2. One can see that μ Cep is slightly metal deficient. The abundance errors of the elements, other than those of the iron peak, are quite large due to small number of measured lines and severe blending.

The random errors rising from using of different lines are presented in Table 2. The systematic effect from the lowering of the effective temperature by $100~{\rm K}$ causes the rise of Fe abundance by $0.1~{\rm dex}$.

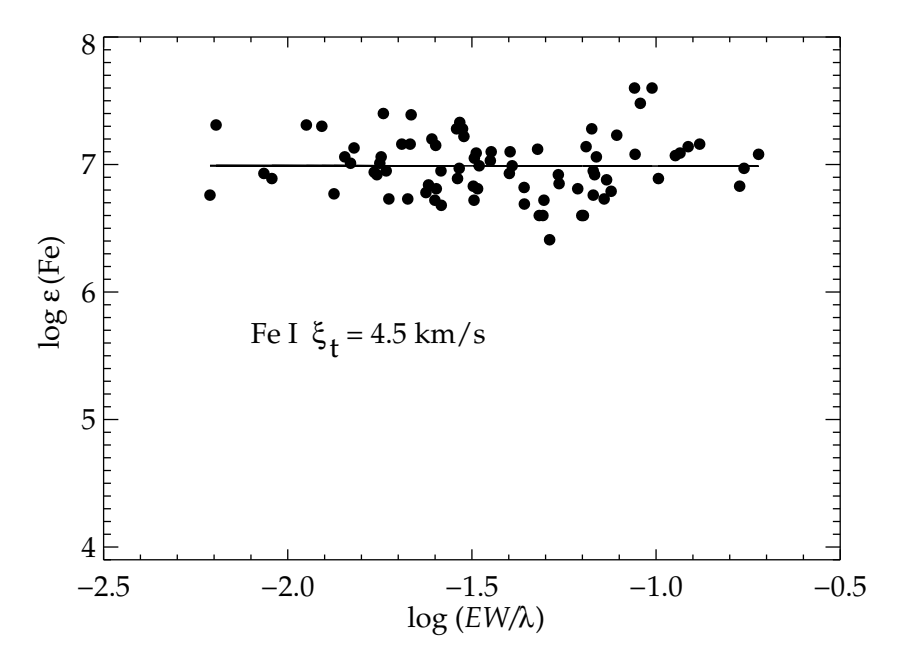


Fig. 2. The dependence of iron abundances on the reduced equivalent widths for all (80) measured Fe I lines. The microturbulent velocity is $\xi_t = 4.5 \text{ km s}^{-1}$.

2.4. The NaID and H α lines

The Na I D lines have composite profile. In Table 3 and Figure 5 the Gaussian decomposition of these lines in the velocity scale is presented. The velocities are derived relative to the radial velocity of the star. For the decomposition the mean spectrum for the period from JD 2451412.5 till JD 2453211.5 was used. The profile was stable during the whole period except of the component 4 which during the first observation was about 20% weaker than in the mean spectrum. The close fit of intensities of the $\rm D_1$ and $\rm D_2$ components points to heavy saturation and excludes further analysis of these lines.

Table 3. Results of the Gaussian decomposition of Na I D lines in the spectrum of μ Cep.

No.	λD_2	EW	v_{\star}	λD_1	EW	v_{\star}
	[nm]	[pm]	$[\mathrm{km/s}]$	[nm]	[pm]	[km/s]
1	588.907	53.6	-42.0	589.506	46.8	-40.8
2	588.944	12.1	-23.1	589.543	19.5	-21.9
3	588.974	51.5	-7.9	589.575	46.3	-5.7
4	589.037	46.5	24.2	589.632	42.5	23.3

The H α line was variable during nearly five years of the used observations. However, the observations were distributed very unevenly in time, and we grouped them with no discernible changes in H α and averaged them. The time between the first observation and the second group is about 3.8 years, then the third and the fourth groups each followed in about a half of year. The time evolution of

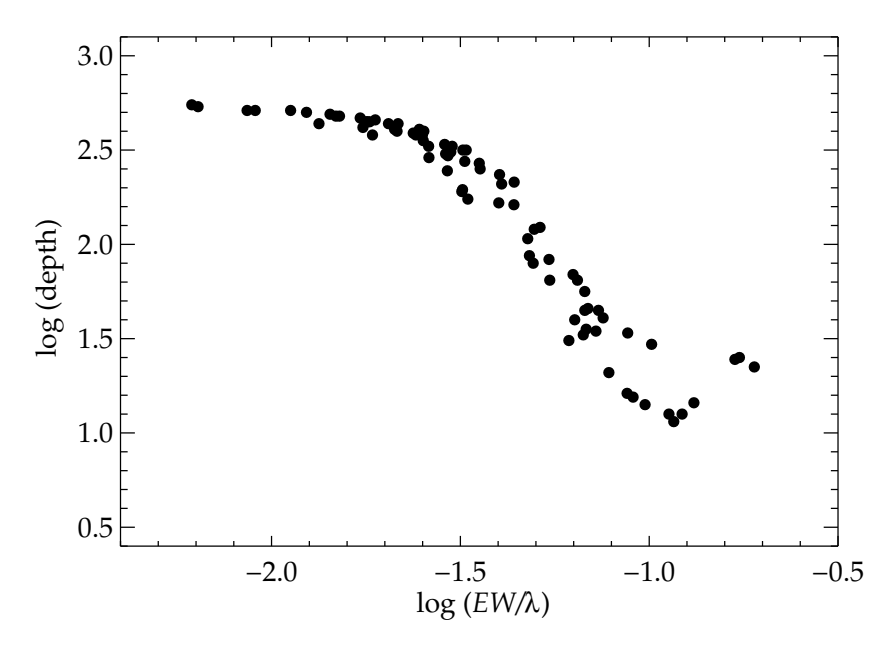


Fig. 3. The dependence of the iron line formation depth on the reduced equivalent widths for all (80) measured Fe I lines.

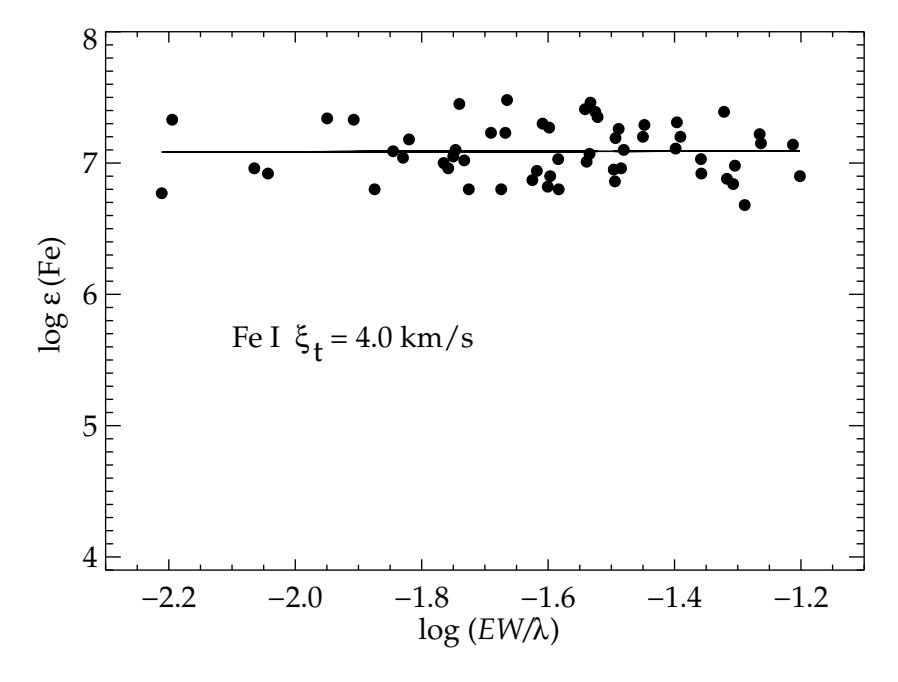


Fig. 4. The same as in Fig. 2 but for 57 weaker lines with $\log(EW/\lambda) \le -1.2$. Here the microturbulent velocity is $\xi_{\rm t} = 4.0~{\rm km\,s^{-1}}$.

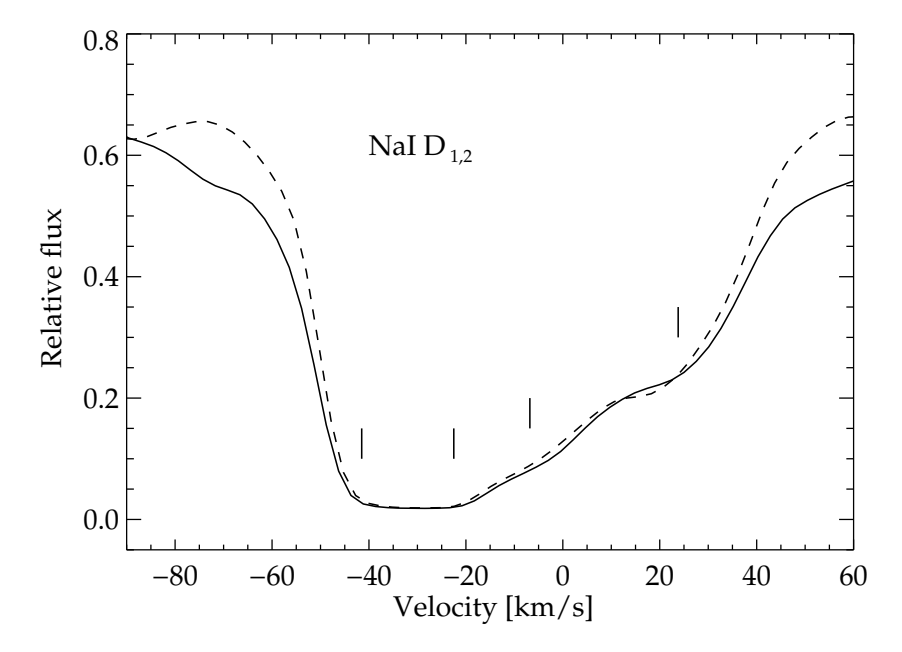


Fig. 5. The Gaussian decomposition of the NaID lines in the velocity scale (D_2 – solid line, D_1 – dashed line). Zero velocity corresponds to the radial velocity of the star. The mean of all used spectra is plotted.

the ${\rm H}\alpha$ line is presented in Figure 6. The line was narrowest during the first observation and its wavelength corresponded then quite well to the radial velocity of the star. In other observations one could follow a gradual widening of the red wing of the line, and for the last observation the widening of the blue wing also. At the same time the central wavelength of the line has also increased. According to the AAVSO light curve of μ Cep, a deep light drop close to the last spectral observation could be present. That drop could be as large as $\Delta V=0.6$ mag, but no direct photometry is available at the time of spectral observations.

3. CONCLUSION

In the spectra of ${\rm H}\alpha$ region of late type giants and supergiants observed by Eaton (1995), metallic lines in the spectra of μ Cep and α Ori are notably wider than in other stars. In this work I found that the line width depends on the line formation depth being larger in outer layers of the stellar atmosphere. The difference in velocities responsible for these line widths is about 20 km s⁻¹. The velocity gradients found by Josselin & Plez (2007) were close to that. The velocities themselves are highly supersonic. This indicates that large granules can be present in the atmosphere of μ Cep. Chivassa et al. (2010) have modeled convection for the Betelgeuse, a close kin of μ Cep, and indeed found that the star is characterized by a granulation pattern composed of convection related granules and large convective cells. At the same time the microturbulent velocity is rather low, (4.0 km s⁻¹). The Fe I lines stronger than $\log(EW/\lambda) \geq -1.2$, which form in the outer layers of the atmosphere, show slightly larger microturbulent velocity, $\xi_{\rm t} = 4.3~{\rm km\,s^{-1}}$.

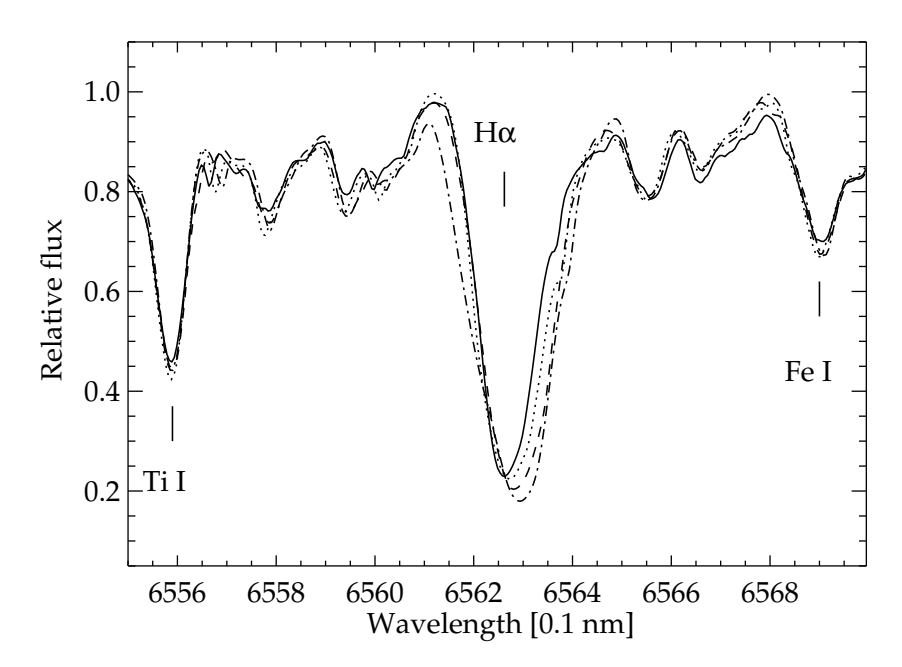


Fig. 6. Profiles of the H α line during four time intervals. On JD 2451421.5 – solid line, from JD 2452787.5 to JD 2452826.5 – dotted line, from JD 2452873.5 to JD 24523051.2 – dashed line and from JD 2453122.6 to JD 2453211.5 – dash-dotted line. The positions of Ti I line at 655.608 nm and Fe I line at 656.922 nm, and the H α position with the radial velocity determined by these two lines, are indicated.

The chemical composition of μ Cep is found to be slightly metal deficient with $[\text{Fe/H}] \approx -0.4$. This leads to somewhat lower ($\sim 100 \text{ K}$) effective temperature than it was assumed earlier. For other elements than of the iron peak the results are very uncertain due to small number of the measured lines.

ACKNOWLEDGMENTS. This research is based on the spectral data retrieved from the ELODIE archive at Observatoire de Haute-Provence and photometry from the AAVSO International Database. I am thankful for the possibility of use these databases.

REFERENCES

Bell R. 1976, private communication

Bessell M. S., Castelli F., Plez B. 1998, A&A, 337, 321

Chiavassa A., Haubois X., Young J. S. et al. 2010, A&A, 515, A12

Eaton J. A. 1995, AJ, 109, 1797

Grevesse N., Noels A., Sauval A. J. 1996, ASP Conf. Ser., 99, 117

Gustafsson B., Edvardson B., Eriksson K. et al. 2003, ASP Conf. Ser., 288, 331

Humphreys R. M. 2007, Rev. Mex. AA, 30, 6

Josselin E., Plez B. 2007, A&A, 469, 671

Kurucz R. 1979, SAO Spec. Report, No. 9

Lambert D. L., Brown J. A., Hinkle K. H., Johnson H. R. 1984, ApJ, 284, 223

Levesque E. M., Massey P., Olsen K. A. G. et al. 2005, ApJ, 628, 973 Massey P., Plez B., Levesque E. M. 2008, ASP Conf. Ser., 412, 3 Moultaka J., Ilovaisky S. A., Prugniel P., Soubrian C. 2004, PASP, 116, 693 Orlov M. Ya. 1967, Soviet Astron., 10, 619 Plez B. 1992, A&AS, 94, 527 Plez B. 1998, A&A, 337, 495 Thevenin F. 1989, A&AS, 77, 137 Thevenin F. 1990, A&AS, 82, 179 Yamashita Y. 1956, PASJ, 8, 142

Yamashita Y. 1965, PASJ, 17, 27